# Atlantic Ocean $CO_2$ uptake reduced by weakening of the meridional overturning circulation

Fiz F. Pérez[1], Herlé Mercier[2], Marcos Vázquez-Rodríguez[1], Pascale Lherminier[3], Anton Velo[1], Paula C. Pardo[1], Gabriel Rosón[4] and Aida F. Ríos[1]

[1] Instituto de Investigaciones Marinas, IIM-CSIC, 36208 Vigo, Spain
[2] CNRS, Laboratoire de Physique des Océans, UMR6523, CNRS, Ifremer, IRD, UBO, Plouzané, France
[3] Ifremer, Laboratoire de Physique des Océans, UMR6523, CNRS, Ifremer, IRD, UBO, Plouzané, France
[4] Faculty of Marine Sciences, University of Vigo, Campus Lagoas-Marcosende, 36200 Vigo, Spain.

Over the last two decades (1990-2006) observations showed a rapid weakening of the oceanic uptake of atmospheric $CO_2$ in the subpolar North Atlantic related to sea-surface warming. At the same time, high-resolution models pointed out a decrease in the Atlantic meridional overturning circulation, which plays a key role in the climate system by redistributing heat, fresh water and $CO_2$ by carrying warm upper waters into northern latitudes and returning cold deep waters southward across the equator Using transoceanic volume, heat and $CO_2$ transports data we analysed the fundamental differences in the physical mechanisms governing the $CO_2$ budget between the subtropical and subpolar North Atlantic regions. We found that the air-sea uptake of anthropogenic $CO_2$ -the $CO_2$ released by human activities- occurs almost exclusively in the subtropical gyre, whereas the subpolar gyre predominantly uptakes natural $CO_2$. Here we show that the decrease in air-sea heat loss linked to the reduction in the meridional overturning circulation, driven by the North Atlantic Oscillation, is the major factor explaining the decline of natural $CO_2$ uptake in the subpolar gyre during the last decade. Furthermore, the concomitant decrease in the anthropogenic $CO_2$ storage rate is primarily attributed to the reduction in the meridional overturning circulation.

Contemporary $CO_2$ uptake from the atmosphere by the global ocean has been estimated at $1.6 \pm 0.9$ $PgC \cdot y^{-1}$ from an observation-based $CO_2$ flux climatology[1] referenced to year 2000. Contemporary atmospheric $CO_2$ consists of a mix of molecularly identical natural and anthropogenic $CO_2$ ($C_{ANT}$). The whole North Atlantic (NA -from the Equator to the Bering Strait, including the Arctic Seas) represents only 13% of the global ocean area and yet annually accounts for about one-third of the contemporary ocean $CO_2$ uptake (0.47 $PgC \cdot y^{-1}$) and has the largest of $C_{ANT}$ storage rates ($0.49 \pm 0.04$ $PgC \cdot y^{-1}$ referenced to 2004) of all oceans[2]. However, air-sea $CO_2$ uptake in the NA is not necessarily predominantly anthropogenic[3,4]. Actually, air-sea $CO_2$ fluxes in the NA result from anthropogenic forcing and progressive northward cooling of the upper limb of the meridional overturning circulation

(MOC). The latter is responsible for the NA uptake of natural $CO_2$ (ref. 5) that would occur even in the absence of the anthropogenic forcing. This air-sea flux of natural $CO_2$ is driven by thermal processes[5] — not biological processes — and has been estimated in 0.31-0.39 $PgC \cdot y^{-1}$ (refs 5,6), which represents roughly three-fourths of the contemporary air-sea $CO_2$ uptake. The remaining uptake (0.08-0.16 $PgC \cdot y^{-1}$) comes from the anthropogenic perturbation, which alone cannot account for the $C_{ANT}$ storage rate of the NA[2]. The additional source of $C_{ANT}$ comes from the northward transport of $C_{ANT}$-laden south-latitude waters[4,7–9] by the upper limb of the MOC.

Air-sea $CO_2$ fluxes in the subpolar and subtropical regions have similar rates (0.27 and 0.22 $PgC \cdot y^{-1}$, referenced to 2000, respectively[1]), but the flux per unit area in the subpolar NA is twice that in the subtropical NA (2.0 vs. 1.0 $mol\text{-}C \cdot m^{-2} \cdot y^{-1}$). At multidecadal time scales, sea surface $pCO_2$ in these regions follow the atmospheric increase[1]. However, these two regions also have contrasting responses to different North Atlantic Oscillation (NAO) periods. Between 1993 and 2006, the $CO_2$ uptake rate in the western subpolar[10] and, more generally, in the subpolar gyre[11] dramatically weakened as evidenced by the rapid increase in sea-surface $pCO_2$ compared to atmospheric $pCO_2$. Changes in the NAO (the index declined from high positive values in the early 1990s to lower values in the early 2000s)[12] and the associated weakening of the northward transport of subtropical water by the North Atlantic Current (NAC) have been identified, using inverse atmospheric $CO_2$ and physical-biological models[13,14], as the main causes for the decrease in $CO_2$ uptake in the subpolar NA. In contrast, in the subtropical NA, $CO_2$ uptake increased during the years with low NAO index[15,16]. There are, however, few observations of $C_{ANT}$ transport reported for different NAO conditions. In addition, numerical models have shown contrasting $CO_2$ uptake responses[14,17] and discrepancies with field data, suggesting that more observations are required to better understand the interactions between ocean circulation and the carbon cycle, in particular regarding the mechanisms governing the exchange, advection and accumulation of $CO_2$.

## $CO_2$ transport by the meridional overturning circulation

The analysis of repeated trans-Atlantic sections at 25ºN showed that the upper limb of the MOC carries 18.7±2.1 Sv (Sv = $10^6$ $m^3 \cdot s^{-1}$) northwards[18] (northward transport is considered positive). Most of this transport occurs through the Gulf Stream and, downstream, through the NAC (Fig. 1). The warm water moving northward in the upper limb of the MOC has high concentrations of $C_{ANT}$ ([$C_{ANT}$]), whereas the cold, deep water moving southward[4,7] has very low [$C_{ANT}$]. This pattern yields net northward transports of heat[19] and $C_{ANT}$ of 1-1.3 PW and 0.19-0.23 $PgC \cdot y^{-1}$ (refs 4, 7), respectively. The overturning and the southward transport of deep water of the MOC happen in the northern NA and Nordic seas, where high wintertime heat loss generates vertical convection and produces cold, fresh and well-ventilated deep waters[20] that are entrained in the deep western boundary current. Recent estimations of the MOC across the repeated A25 section (Greenland to Portugal; Fig. 1) showed slightly weaker mass transports[21,22] (12-18.5 Sv) than at 25ºN. The upper and lower limbs of the MOC showed contrasting temperatures and [$C_{ANT}$] (Fig 1b, see Methods for details on $C_{ANT}$ computations), but both properties are positively correlated. The small westward increase in [$C_{ANT}$] at constant temperature indicates recent ventilation of the western side of the section. In the surface layer, [$C_{ANT}$] is close to saturation. East of the NAC, the low values (< 10 $\mu mol.kg^{-1}$) in deep waters create a larger vertical gradient of $C_{ANT}$ between the surface and the deep ocean than to the west of the NAC, *i.e.* in the subpolar region, where the Labrador Sea Water (LSW), the Denmark Strait Overflow Water and the Iceland-Scotland Overflow Water show moderate [$C_{ANT}$].

Numerical models have shown that NAO conditions influence air-sea $CO_2$ uptake in the NA[13] by modulating the strength with which the NAC carries subtropical waters into the subpolar gyre[14]. However, these results have not been confronted with measurements of volume, heat and $CO_2$ transports due to the lack of observations during different NAO conditions. We examined several occupations of the A25 Greenland-Portugal section (Fig. 1a) conducted in August 1997 (FOUREX cruise) and in June 2002, 2004 and 2006 (OVIDE cruises). The year 1997 came after an unusually long high NAO period followed by a period of lower NAO between 2002 and 2006. The A25 cruise was specifically designed to run perpendicularly across the main NA currents (the different branches of the NAC and the boundary currents linked to the topography) in order to minimize the transports due to eddies[23]. Measurements from these cruises were used to calculate $MOC_\sigma$ transport[21,22,24], taking $\sigma_1$ (density anomaly referenced to 1000 dbar) as the vertical coordinate (Fig. 2). $MOC_\sigma$, varied from 20.5±2.2 Sv in 1997 to the average value of 14.6±1.7 Sv for the 2002-2006 period (see Methods and Supplementary Information for details on the removal of the seasonal cycle and the computation of the uncertainties). When integrated from Greenland to Portugal along constant $\sigma_1$-lines, heat and $C_{ANT}$ transports resemble the vertical profiles of the overturning circulation (Fig. 2). Volume, heat and $C_{ANT}$ transport profiles are highly correlated ($0.92>r^2>0.89$), because the upper limb of the MOC transports warmer waters with higher [$C_{ANT}$] than the lower limb. On average, the net volume transport is negligible, and there is a net northward transport of heat (0.59±0.09 PW) and $C_{ANT}$ (0.092±0.010 $PgC \cdot y^{-1}$). In 1997, the circulation showed a strong southward volume transport at intermediate levels ($32.4<\sigma_1<32.5$) that corresponds to the layer of the classical LSW (Fig. 2). On the other hand, during the lower NAO period, the southward volume transport was slightly stronger in the layer of the upper LSW ($32.2<\sigma_1<32.3$)[20]. In addition, the upper limb of $MOC_\sigma$ ($\sigma_1<32.1$) showed a stronger transport in 1997 than in 2002-2006 (Fig. 2a), which is attributed to the NAC variability[24]. The heat and $C_{ANT}$

transports in 2002-2006 (0.41±0.06 PW and 0.074±0.009 $PgC\cdot y^{-1}$) were lower than in 1997 (0.76±0.09 PW and 0.110±0.012 $PgC\cdot y^{-1}$). Most remarkably, although the weakening of $MOC_\sigma$ and of $C_{ANT}$ transport were very similar (29% and 33%, respectively), heat transport underwent a more dramatic reduction (46%) between 1997 and 2002-2006. This contrasting behavior of volume and heat transports agrees with results from high-resolution circulation models[25]. We will treat the observations obtained in 1997 as a case study of circulation linked to a high NAO period, as opposed to the measurements obtained during 2002-2006 that were associated with a low/neutral NAO period.

**Anthropogenic $CO_2$ budget of the North Atlantic**

The $C_{ANT}$ budget of any oceanic region is the result of the balance between lateral advection, air-sea fluxes and storage rates. Hereinafter, we will refer to the NA as the region extending from 25ºN to the Bering Strait. We calculated the NA $C_{ANT}$ budget referenced to 2004 from updated datasets and for four different subregions or boxes (Fig. 3). In the subtropical box, the $C_{ANT}$ storage rate was computed as described in the Methods section, while the estimates in other boxes were obtained from the literature (Supplementary Information). For the NA, we obtained a storage rate of 0.386±0.012 $PgC\cdot y^{-1}$ (0.95±0.05 $mol\text{-}C\cdot m^{-2}\cdot y^{-1}$) consistent with previous results (0.39±0.02 $PgC\cdot y^{-1}$, referenced to 2004; ref. 26). The $C_{ANT}$ transports at 25°N (refs 4,7) were updated from 1992 and 1998 to 2004, resulting on a mean value of 0.25±0.05 $PgC\cdot y^{-1}$ (Methods section) that is consistent with a long term average MOC (ref. 18). Comparatively, $C_{ANT}$ transport in the Bering Strait is low (0.008±0.003 $PgC\cdot y^{-1}$)[7,26]. Closing the $C_{ANT}$ budget in the NA, an air-sea $C_{ANT}$ flux of 0.13±0.05 $PgC\cdot y^{-1}$ was inferred. This estimate is compatible with the value of 0.17±0.06 $PgC\cdot y^{-1}$ (rescaled to 2004) derived from $\delta^{13}C$ observations[9]. Overall, these results indicate that the net advective transports contribute to 65±13% of the NA $C_{ANT}$ storage rate (Fig. 3). Importantly, our observation-based estimate of the contribution of lateral transports to the $C_{ANT}$ storage rate is larger than the 30% obtained by ocean inversions that combine $C_{ANT}$ observations with transports and mixing from GCMs (ref. 26). By way of contrast, our result is consistent with a biogeochemical model[27] that predicted larger northward $C_{ANT}$ transports than ocean inversions in the NA. Subtracting our estimate of air-sea $C_{ANT}$ flux from the contemporary $CO_2$ uptake for the NA (0.49 $PgC \cdot y^{-1}$; ref. 1), we obtained a natural $CO_2$ uptake of 0.36 $PgC \cdot y^{-1}$, thereby corroborating independent estimates[5,6]. The air-sea $C_{ANT}$ flux represents about 26% of the contemporary air-sea $CO_2$ uptake, which is much smaller than the 63% obtained from oceanic inversions[3]. The relevance of our result is that the air-sea $C_{ANT}$ and natural $CO_2$ uptake estimates from the $C_{ANT}$ budget are consistent with independent $^{13}C/^{12}C$ observations[9] and with other estimates of the air-sea natural $CO_2$ uptake[5,6].

The $C_{ANT}$ storage rate estimated for the subtropical box is $0.280 \pm 0.011$ $PgC \cdot y^{-1}$ ($1.41 \pm 0.05$ mol-$C \cdot m^{-2} \cdot y^{-1}$). So the subtropical box contributes 73% of the NA $C_{ANT}$ storage rate, even though it represents only 49% of the NA area. By closing the $C_{ANT}$ budget for this box (Fig. 3), we inferred an air-sea $C_{ANT}$ uptake of $0.12 \pm 0.05$ $PgC \cdot y^{-1}$ ($0.60 \pm 0.25$ mol-$C \cdot m^{-2} \cdot y^{-1}$). Here, the air-sea $C_{ANT}$ flux is predominant in the contemporary air-sea $CO_2$ flux (1.0 mol-$C \cdot m^{-2} \cdot y^{-1}$). It represents 92% of the NA air-sea $C_{ANT}$ uptake. In contrast, in the subpolar box, the $C_{ANT}$ storage rate per unit area ($0.99 \pm 0.06$ mol-$C \cdot m^{-2} \cdot y^{-1}$) amounts to ~70% of that in the subtropical box[28]. To derive the $C_{ANT}$ budget for the subpolar box, the $C_{ANT}$ lateral transport over the Nordic sills ($0.063 \pm 0.019$ $PgC \cdot y^{-1}$) was calculated from available volume transports[22,29] and from [$C_{ANT}$] estimated from water mass ages and mixing models[30] (Supplementary Information). Then, the air-sea $C_{ANT}$ flux was estimated at $0.016 \pm 0.012$ $Pg\text{-}C \cdot y^{-1}$, which represents 35% of the $C_{ANT}$ storage rate in this box. The air-sea $C_{ANT}$ flux per unit area in the subpolar box ($0.36 \pm 0.25$ mol-$C \cdot m^{-2} \cdot y^{-1}$) is about 60% of the subtropical box which gives to the subtropical box a prevailing role in $C_{ANT}$ uptake. Furthermore, the contemporary air-sea $CO_2$ uptake per unit area (2.0 mol-C·m$^{-2}$·y$^{-1}$) in the subpolar box is 5 times higher than the air-sea $C_{ANT}$ uptake. This means that the natural component largely prevails over the anthropogenic component in the subpolar box. Interestingly, this result is in contrast with the subtropical box, where the air-sea anthropogenic flux is the major component (~60%).

The net heat and $C_{ANT}$ transports flowing into the Nordic Seas reach 0.25±0.05 PW and 0.063±0.019 PgC·y$^{-1}$, respectively (Fig. 3, Supplementary Information). The $C_{ANT}$ lateral transport almost fully accounts for the $C_{ANT}$ storage rate in the Nordic[31] and Arctic Seas[32] meaning that air-sea $C_{ANT}$ fluxes are practically zero (Fig. 3). Analyses based on $^{13}C/^{12}C$ measurements[33,34] have determined that the upper waters entering the Nordic Seas are saturated with $C_{ANT}$, preventing any further $C_{ANT}$ uptake from the atmosphere and possibly causing outgassing due to the decline in buffering capacity. The strong air-sea heat loss in the Nordic and Arctic Seas actually drives the uptake of natural $CO_2$, as corroborated by observations in climatological analyses[1] that indicate a high air-sea $CO_2$ uptake (2.0 mol-C·m$^{-2}$·y$^{-1}$) north of 50ºN. In summary, while heat loss causes a strong natural $CO_2$ uptake in the Nordic and Arctic regions, the low anthropogenic component is less affected by the air-sea heat fluxes.

**North Atlantic oscillation impact on $CO_2$ fluxes**

The subpolar gyre is a remarkably rapid entrance portal for $C_{ANT}$ into the deep ocean due to deep convection. In the early 1990s, the highly positive NAO period coincided with exceptional convection activity in the Labrador[20,35] and Irminger[36] Seas. Between 1997 and 2003, lower LSW formation rates prompted a decrease of 20 mol-C·m$^{-2}$ in the $C_{ANT}$ inventory, as inferred from chlorofluorocarbon data[37]. In the subpolar box, the $C_{ANT}$ storage rate dropped from 0.083±0.008 during high NAO conditions in 1997 to 0.026±0.004 PgC·y$^{-1}$ during the 2002-2006 low NAO period[28]. Hence, $C_{ANT}$ storage rates per unit area were nearly three times lower during low NAO than high NAO periods

(Fig. 4). The decrease in northward $C_{ANT}$ transport (Fig. 4) that followed the high-to-low NAO transition (from 0.110 to 0.074 $PgC \cdot y^{-1}$) is strongly related to the weakening of the intensity of the MOC (from 20.5±2.2 to 14.6±1.7 Sv). Most remarkably, the converging $C_{ANT}$ lateral transports in the subpolar box decreased from 0.053±0.021 to 0.011±0.020 $PgC \cdot y^{-1}$. In these estimations, we assumed that the volume transport over the Nordic sills was constant, as suggested by observations[29], and [$C_{ANT}$] was time-rescaled using a rate of increase of 1.6% $y^{-1}$ (Supplementary Information). After these calculations, the inferred air-sea $C_{ANT}$ flux for the subpolar region was 0.53±0.22 $mol\text{-}C \cdot m^{-2} \cdot y^{-1}$ during the high NAO period and 0.33±0.25 $mol\text{-}C \cdot m^{-2} \cdot y^{-1}$ during the low NAO period. During the low NAO period, the $C_{ANT}$ storage rate decreased due to the decrease in $C_{ANT}$ lateral transport associated with the weakening of the MOC. Our results also suggest that this decrease was associated with a weakening in the air-sea $C_{ANT}$ uptake.

The variability of the air-sea $CO_2$ flux in the subpolar gyre has already been described, modeled and discussed in regard to NAO variability[13,14,38,39]. In the north-western subpolar gyre, a reduction in the contemporary air-sea $CO_2$ flux of ~1.2 $mol\text{-}C \cdot m^{-2} \cdot y^{-1}$ was observed between 1993-94 and 2003-05 (refs 11, 38) and numerical simulation linked it to the weakening of the advection of subtropical waters with low total inorganic $CO_2$ ($C_T$) into the subpolar gyre[14]. This weakening is in agreement with our results (Fig. 4). During high NAO periods, heat loss increased[40], favouring the decrease in the surface $pCO_2$. The opposite is true during low NAO periods. Assuming a constant heat flux of 0.25±0.05 PW over the sills[29], we inferred, from the heat budget, a heat loss that is 1.5 to 3 times higher during high NAO than during low NAO periods (Fig. 4). Using the relationship between heat loss and natural $CO_2$ flux (see Methods), we inferred a decrease in the air-sea flux of natural $CO_2$ of 3.0±1.0 to 1.7±1.0 $mol\text{-}C \cdot m^{-2} \cdot y^{-1}$ (0.13 to 0.05 $PgC \cdot y^{-1}$, Fig. 4). This estimate is compatible with the rate of decrease in air-sea $CO_2$ fluxes in the subpolar gyre (2.3 to 1.0 $mol\text{-}C \cdot m^{-2} \cdot y^{-1}$) reported from surface observations[39]. Most importantly, this result strongly suggests that variability in the air-sea flux of natural $CO_2$ over the subpolar gyre responds to variability in the advection of subtropical waters with low [$C_T$] and can be determined from the air-sea heat flux.

A possible explanation for the contrasting behaviour of the subtropical and subpolar regions lies in the origin of the water masses crossing the Florida Strait where ~45% of the volume transport comes from the South Atlantic as warm and intermediate waters[41] with low [$C_{ANT}$] (ref. 4). These low [$C_{ANT}$] waters are part of the upper limb of the MOC and reach $C_{ANT}$ saturation levels on their path to the subpolar gyre. They incorporate about 0.08 $PgC \cdot y^{-1}$, which represents two thirds of the air-sea $C_{ANT}$ flux in the subtropical box and contributes to the local response to anthropogenic forcing (Fig. 3). This explains why the air-sea $C_{ANT}$ flux in the subtropical region is higher than that observed in the subpolar region. Furthermore, the intermediate water flowing through the Florida Strait is oversaturated with natural $CO_2$ (~30 $\mu mol \cdot kg^{-1}$) due to biological remineralization[4]. This allows the waters in the upper limb of the MOC to remain $CO_2$-saturated with low additional atmospheric uptake, despite the ~7ºC cooling undergone as they travel through the subtropical box, thereby explaining the low natural air-sea $CO_2$ flux in this box.

In summary, our results give a coherent and observation-based understanding of the $CO_2$ budget in NA regions. Our analysis provides evidence that the air-sea $C_{ANT}$ flux contribution to the $C_{ANT}$ storage and to the total air-sea $CO_2$ flux in the NA is lower than expected from ocean inversions. Advection is the main contribution to the $C_{ANT}$ storage rate north of 25ºN. Practically, the entire air-sea $C_{ANT}$ uptake in the NA occurs in the subtropical region, where the contemporary air-sea $CO_2$ flux is mainly anthropogenic, whereas the natural component predominates in the subpolar region. The high-to-low NAO transition was followed by a decrease in the heat and $C_{ANT}$ transports into the subpolar region due to the weakening of the MOC and the simultaneous decrease in the $C_{ANT}$ storage rate.

Because the anthropogenic contribution is a minor component of the contemporary air-sea $CO_2$ uptake in the subpolar region, we attribute the weakening of the contemporary air-sea $CO_2$ uptake to the decrease in natural $CO_2$ uptake. Our estimate of the decrease in natural $CO_2$ uptake inferred from the heat budget is in agreement with independent surface observations.

Finally, our study suggests that the long-term prediction of a reduction in the intensity of the MOC would be a positive climate-carbon feedback leading to a decrease in the $C_{ANT}$ storage. Concomitant air-sea heat loss reduction may lead to a decrease in the abiotic component of the natural $CO_2$ uptake, which would be an even more important feedback.

## Methods

**$C_{ANT}$ estimations.** [$C_{ANT}$] was computed using the back-calculation $\varphi C_T^o$ method[42,43] with an overall uncertainty of ±5.2 µmol $kg^{-1}$. [$C_{ANT}$] in the subtropical region was estimated using the gridded CARINA dataset [44] and applying the $\varphi C_T^o$, TrOCA[45] and TTD[46] methods. $C_{ANT}$ storage rates obtained from each of these methods were in good agreement. The final $C_{ANT}$ storage rate and its uncertainty for the subtropical region were calculated as the mean and the standard deviation of $C_{ANT}$ storage rates obtained from each method. For the subpolar, Nordic and Arctic boxes, the storage rates were from refs 28, 31 and 47, respectively. Additional details are provided in the Supplementary Information.

**Transport computations across A25**. Absolute geostrophic currents were estimated using an inverse model constrained by subsurface ADCP (Acoustic Doppler Current Profiler) measurements and an overall mass conservation constraint[21,22,24]. The absolute velocity field is consistent with independent altimetry measurements[24] and estimates of the western boundary current transport[48] at the time of the OVIDE cruises. They are representative of the month of the cruise[23] and the seasonal variability was removed as explained in the Supplementary Information. Heat and $C_{ANT}$ transports were calculated from current velocities perpendicular to the sections and from the potential temperature and $C_{ANT}$ fields, respectively. The uncertainties of the MOC, heat and $C_{ANT}$ transports were estimated to be ±2 Sv, 0.05 PW and 0.014 $PgC \cdot y^{-1}$, respectively (see online Supplementary Information for full calculation details).

The errors of the mean transports (volume, heat or $C_{ANT}$) across the A25 section were calculated as the standard deviation of the transport values divided by the square root of the number of transport values included in the estimate. Since only one transport estimate was available for the high NAO conditions, the error equals the standard deviation of the transports between 1997 and 2006, after removing a linear trend.

**$C_{ANT}$ transport at 25°N.** We used the estimates of $C_{ANT}$ transports across 25ºN reported in refs 4 and 7 that were respectively obtained from hydrographic cruises carried out in 1992 and 1998 and from $C_{ANT}$ estimates based on a classic back-calculation method and on the C* method. We rescaled both estimates to year 2004 by removing the effect of the inter-annual variability of the MOC in $C_{ANT}$ transports along 25ºN. In addition, we corrected the MOC estimates for their intra-annual variability. The resulting value obtained after the rescaling was 0.25±0.05 $PgC \cdot y^{-1}$. Details on these computations and the uncertainty estimates are given in the Supplementary Information.

**Relationship between air-sea fluxes of heat and natural $CO_2$.** The linear regression of natural $C_T$ transports versus heat transports reported in Supplementary Table 4 for the A25 line has a slope of -0.56±0.10 $PgC \cdot y^{-1}$ per PW ($p < 0.05$). Assuming that the variability of heat and natural $C_T$ transports over the sills and of accumulative terms are negligible[29,49], this slope can be interpreted as a relationship between the air-sea flux of natural $CO_2$ and the air-sea heat loss in the subpolar box. In the Nordic seas, a similar relationship is found between air-sea flux of natural $CO_2$ and air-sea heat loss. Using the mean value of the observed air-sea $CO_2$ uptake (0.09 ± 0.01 and 0.11 ± 0.06 $PgC \cdot y^{-1}$ as reported in refs 1 and 50, respectively) and the heat loss given in Fig. 3, we obtained a value of -0.5±0.1 PgC·yr$^{-1}$ of air-sea flux per PW of heat loss in the Nordic seas. This relationship can also be applied to the natural $CO_2$ air-sea fluxes of the Nordic Seas, since here the $C_{ANT}$ air-sea flux is negligible, as shown in Fig. 3.

## References


1. Takahashi, T. *et al.* Climatological mean and decadal change in surface ocean $pCO_2$, and net sea-air $CO_2$ flux over the global oceans. *Deep-Sea Res. II* **56,** 554–577 (2009).
2. Sabine, C. L. *et al.* The oceanic sink for anthropogenic $CO_2$. *Science* **305**, 367–371 (2004).
3. Gruber, N. *et al.* Oceanic sources, sinks, and transport of atmospheric $CO_2$. *Glob. Biogeochem. Cycles* **23,** (2009).
4. Rosón, G., Rios, A. F., Pérez, F. F., Lavin, A. & Bryden, H. L. Carbon distribution, fluxes, and budgets in the subtropical North Atlantic Ocean (24.5ºN). *J. Geophys. Res.***108,** 3144 (2003).
5. Keeling, R. F. & Peng, T.-H. Transport of Heat, $CO_2$ and $O_2$ by the Atlantic's Thermohaline Circulation. *Phil. Trans. R. Soc. Lond. B* **348,** 133–142 (1995). (*1995*) *348*, *133-142* **.**
6. Mikaloff-Fletcher, S. E. *et al.* Inverse estimates of the oceanic sources and sinks of natural $CO_2$ and the implied oceanic carbon transport. *Glob. Biogeochem. Cycles* **21,** GB1010, 19 PP. (2007).
7. Macdonald, A. M., Baringer, M. O., Wanninkhof, R., Lee, K. & Wallace, D. W. R. A 1998–1992 comparison of inorganic carbon and its transport across 24.5°N in the Atlantic. *Deep-Sea Res. II* **50,** 3041–3064 (2003).
8. Álvarez, M., Ríos, A. F., Pérez, F. F., Bryden, H. L. & Rosón, G. Transports and budgets of total inorganic carbon in the subpolar and temperate North Atlantic. *Glob. Biogeochem. Cycles* **17,** 1002 (2003).

9. Quay, P. *et al.* Anthropogenic $CO_2$ accumulation rates in the North Atlantic Ocean from changes in the $^{13}C/^{12}C$ of dissolved inorganic carbon. *Glob. Biogeochem. Cycles* **21,** GB1009 (2007).
10. Metzl, N. *et al.* Recent acceleration of the sea surface $fCO_2$ growth rate in the North Atlantic subpolar gyre (1993–2008) revealed by winter observations. *Glob. Biogeochem. Cycles* **24,** GB4004 (2010).
11. Watson, A. J. *et al.* Tracking the Variable North Atlantic Sink for Atmospheric $CO_2$. *Science* **326,** 1391–1393 (2009).
12. *The Hurrell NAO winter index is computed as the difference of surface atmospheric pressure between Iceland and Azores (timeseries values available at www.cgd.ucar.edu/cas/jhurrell/indices.html. In the early 90s (1989–1995) the 5-year mean ± standard deviation of this index was 3.3±0.8 indicating a high phase of the NAO. A low NAO phase period followed during the years 2002–2006, when the index value dropped to −0.1±0.6. Year1996 is characterized by negative NAO, and 1997 to 2000 by moderate positive NAO. This pattern is also observed when NAO index from SLP is computed in winter months.*
13. Patra, P. K. *et al.* Interannual and decadal changes in the sea-air $CO_2$ flux from atmospheric $CO_2$ inverse modeling. *Glob. Biogeochem. Cycles* **19,** GB4013 (2005).
14. Thomas, H. *et al.* Changes in the North Atlantic Oscillation influence $CO_2$ uptake in the North Atlantic over the past 2 decades. *Glob. Biogeochem. Cycles* **22,** GB4027 (2008).
15. Gruber, N., Keeling, C. D. & Bates, N. R. Interannual Variability in the North Atlantic Ocean Carbon Sink. *Science* **298,** 2374 –2378 (2002).
16. Bates, N. R. Interannual variability of the oceanic $CO_2$ sink in the subtropical gyre of the North Atlantic Ocean over the last 2 decades. *J. Geophys. Res.* **112,** C09013, 26 PP. (2007).

17. Ullman, D. J., McKinley, G. A., Bennington, V. & Dutkiewicz, S. Trends in the North Atlantic carbon sink: 1992-2006. *Glob. Biogeochem. Cycles* **23,** (2009).

18. Kanzow, T. *et al.* Seasonal Variability of the Atlantic Meridional Overturning Circulation at 26.5°N. *J. Clim.* **23,** 5678–5698 (2010).

19. Bryden, H. L., Longworth, H. R. & Cunningham, S. A. Slowing of the Atlantic meridional overturning circulation at 25° N. *Nature* **438,** 655–657 (2005).

20. Yashayaev, I. & Dickson, B. Transformation and Fate of Overflows in the Northern North Atlantic. *Arctic–Subarctic Ocean Fluxes* 505–526 (2008).

21. Lherminier, P. *et al.* Transports across the 2002 Greenland-Portugal Ovide section and comparison with 1997. *J. Geophys. Res.* **112,** C07003 (2007).

22. Lherminier, P. *et al.* The Atlantic Meridional Overturning Circulation and the subpolar gyre observed at the A25-OVIDE section in June 2002 and 2004. *Deep-Sea Res. I* **57,** 1374–1391 (2010).

23. Treguier, A. M. *et al.* The North Atlantic Subpolar Gyre in Four High-Resolution Models. *J. Phys. Oceanogr.* **35,** 757–774 (2005).

24. Gourcuff, C., Lherminier, P., Mercier, H. & Le Traon, P. Y. Altimetry combined with hydrography for ocean transport estimation. *J. Atmos. Oceanic. Technol.* **29,** 1324-1336 (2011).

25. Böning, C. W., Scheinert, M., Dengg, J., Biastoch, A. & Funk, A. Decadal variability of subpolar gyre transport and its reverberation in the North Atlantic overturning.*Geophys. Res.Lett.***33,** L21S01 (2006).

26. Mikaloff-Fletcher, S. E. M. *et al.* Inverse estimates of anthropogenic $CO_2$ uptake, transport, and storage by the ocean. *Glob. Biogeochem. Cycles* **20,** GB2002 (2006).

27. Tjiputra, J. F., Assmann, K. & Heinze, C. Anthropogenic carbon dynamics in the changing ocean. *Ocean Sci.* doi:10.5194/os-6-605-2010 (2010).

28. Pérez, F. F. *et al.* Trends of anthropogenic $CO_2$ storage in North Atlantic water masses. *Biogeosciences*, doi:10.5194/bg-7-1789-2010. (2010).

29. Hansen, B. & Østerhus, S. North Atlantic–Nordic Seas exchanges. *Prog. Oceanogr.* **45,** 109–208 (2000).

30. Tanhua, T., Olsson, K. A. & Jeansson, E. Tracer Evidence of the Origin and Variability of Denmark Strait Overflow Water. *Arctic–Subarctic Ocean Fluxes* 475–503 (2008).

31. Jutterström, S. *et al.* Evaluation of anthropogenic carbon in the Nordic Seas using observed relationships of N, P and C versus CFCs. *Prog. Oceanogr.* **78,** 78–84 (2008).

32. Anderson, L. G., Olsson, K. & Chierici, M. A carbon budget for the Arctic Ocean. *Glob. Biogeochem. Cycles* **12,** 455–465 (1998).

33. Olsen, A. *et al.* Magnitude and Origin of the Anthropogenic $CO_2$ Increase and the $^{13}C$ Suess Effect in the Nordic Seas since 1981. *Glob. Biogeochem. Cycles* **20,** GB3027 (2006).

34. Körtzinger, A., Quay, P. D. & Sonnerup, R. E. Relationship between anthropogenic $CO_2$ and the 13C Suess effect in the North Atlantic Ocean. *Glob. Biogeochem. Cycles* **17,** 1005 (2003).

35. Kieke, D. *et al.* Changes in the pool of Labrador Sea Water in the subpolar North Atlantic. *Geophys. Res. Lett.* **34,** L06605 (2007).

36. Våge, K., Pickart, R. S., Moore, G. W. K. & Ribergaard, M. H. Winter Mixed Layer Development in the Central Irminger Sea: The Effect of Strong, Intermittent Wind Events. *J. Phys. Oceanogr.* **38,** 541–565 (2008).

37. Steinfeldt, R., Rhein, M., Bullister, J. L. & Tanhua, T. Inventory changes in anthropogenic carbon from 1997–2003 in the Atlantic Ocean between 20°S and 65°N. *Glob. Biogeochem. Cycles* **23,** GB3010 (2009).

38. Corbière, A., Metzl, N., Reverdin, G., Brunet, C. & Takahashi, T. Interannual and decadal variability of the oceanic carbon sink in the North Atlantic subpolar gyre. *Tellus B* **59,** 168–178 (2007).

39. Schuster, U. & Watson, A. J. A variable and decreasing sink for atmospheric $CO_2$ in the North Atlantic. *J. Geophys. Res.* **112,** C11006 (2007).

40. Visbeck, M. *et al.* The ocean's response to North Atlantic Oscillation variability. *Geophysical Monograph Series* **134,** 113–145 (2003).

41. Schmitz, W. J. & Richardson P. L. On the sources of the Florida Current. *Deep-Sea Research* **38, Suppl. 1,** S389–S409 (1991).

42. Pérez, F. F. *et al.* Temporal variability of the anthropogenic $CO_2$ storage in the Irminger Sea. *Biogeosciences*, doi:10.5194/bg-5-1669-2008 (2008).

43. Vázquez-Rodríguez, M. *et al.* Anthropogenic carbon distributions in the Atlantic Ocean: data-based estimates from the Arctic to the Antarctic. *Biogeosciences* doi:10.5194/bg-6-439-2009 (2009).

44. Velo, A. *et al.* A multiparametric method of interpolation using WOA05 applied to anthropogenic $CO_2$ in the Atlantic. *Sci. Mar.***74,** 21–32 (2010).

45. Touratier, F., Azouzi, L. & Goyet, C. CFC-11, $\Delta^{14}C$ and $^{3}H$ tracers as a means to assess anthropogenic $CO_2$ concentrations in the ocean. *Tellus B* **59,** 318–325 (2007).

46. Waugh, D. W., Hall, T. M., McNeil, B. I., Key, R. & Matear, R. J. Anthropogenic $CO_2$ in the oceans estimated using transit time distributions. *Tellus B* **58,** 376–389 (2006).

47. Tanhua, T. *et al.* Ventilation of the Arctic Ocean: Mean ages and inventories of anthropogenic $CO_2$ and CFC-11. *J. Phys. Oceanogr.* **114,** C01002 (2009).

48. Daniault, N., Lherminier, P. & Mercier, H. Circulation and Transport at the Southeast Tip of Greenland. *J. Phys. Oceanogr.* **41,** 437–457 (2011).

49. Jeansson, E. *et al.* The Nordic Seas carbon budget: Sources, sinks, and uncertainties. *Glob. Biogeochem. Cycles* **25,** GB4010,16 PP. (2011).

50. Skjelvan, I. *et al.* A review of the inorganic carbon cycle of the Nordic Seas and Barents Sea. *The Nordic Seas: An Integrated Perspective Oceanography, Climatology, Biogeochemistry, and Modeling* **158,** 157–175 (2005).

Correspondence to: F. F. Pérez (fiz.perez@iim.csic.es).

**Acknowledgements**

This work was supported by the Spanish Ministry of Sciences and Innovation and co-founded by the Fondo Europeo de Desarrollo Regional 2007-2012 (FEDER) through the CATARINA project (CTM2010-17141) and through EU FP7 project CARBOCHANGE “Changes in carbon uptake and emissions by oceans in a changing climate” which received funding from the European Commission’s 7th Framework Programme EU under grant agreement no. 264879. The OVIDE research project was co-funded by the IFREMER, CNRS/INSU and LEFE. H.M. was supported by CNRS and PL by IFREMER. M.V-R. was funded by CSIC I3P Predoctoral Grant program (I3P-BPD2005).

**Author Contributions**

All authors contributed extensively to the work presented in this paper. F.F.P., H.M. and A.F.R. designed the research. F.F.P., H.M., M.V-R, A.V., P.L. and A.F.R. analysed the physical and chemical data. H.M. and P.L. estimated the currents and thermohaline fields. F.F.P., M.V-R, A.V. and G.R. determined the anthropogenic $CO_2$ concentrations and storage rates. H.M., F.F.P., P.L. and A.F.R. estimated the uncertainties. F.F.P., H.M., M.V-R., P.C.P. and A.F.R wrote the paper. All authors discussed the results and implications and commented on the manuscript at all stages.

**Author Information**

The authors declare no competing financial interests. Supplementary Information is linked to the online version of the paper at www.nature.com/nature. Reprints and permissions information is available online at http://www.nature.com/nature/reprints. Correspondence and request for materials should be addressed to F.F.P.

## Figure Legends

**Figure 1 | Circulation and $C_{ANT}$ in the North Atlantic. a)** $C_{ANT}$ storage rates (mol-C·m$^{-2}$·y$^{-1}$) and the main currents and water masses participating in the MOC (black line: North Atlantic Current (NAC), Gulf Stream (GS); grey line: Labrador Sea Water –LSW-, white lines: Denmark Strait and Iceland-Scotland Overflow Waters -DSOW and ISOW). The 25ºN, FOUREX and OVIDE section tracks are indicated (blue dotted lines); **b)** Vertical distribution of [$C_{ANT}$] (µmol·kg$^{-1}$) during the OVIDE 2004 cruise. Potential temperature (ºC; white lines) and the isopycnal $\sigma_1$ =32.10 (solid black line) separating the upper and lower limbs of MOC are also shown.

**Figure 2 | Integrated transports of volume, heat and $C_{ANT}$ across the A25 section (Greenland - Portugal) in 0.01 density bins. a)** Volume transport ($10^6$ m$^3$ s$^{-1}$); **b)** Heat transport (PW); **c)** $C_{ANT}$ transport (kmol s$^{-1}$). Color lines refer to years 1997 (grey), 2002 (yellow), 2004 (red) and 2006 (blue). The $\sigma_1$ = 32.10 horizon (solid black horizontal lines) represents the boundary between the upper and lower limbs of the MOC. NAC = North Atlantic Current, uLSW = upper Labrador Sea Water, cLSW = classical Labrador Sea Water.

**Figure 3 | $C_{ANT}$ budget in the North Atlantic referred to 2004.** The upper box represents the NA and the lower boxes represent the four sub-regions. The horizontal arrows show the lateral transports of $C_{ANT}$ in PgC·y$^{-1}$ (blue font) and heat transports in PW (maroon font). The black numbers in the boxes are the $C_{ANT}$ storage rates in PgC·y$^{-1}$. The vertical arrows show the anthropogenic (numbers in blue font) and contemporary (red font) air-sea $CO_2$ fluxes in PgC·y$^{-1}$. Errors appear in grey font. The surface area (m$^2$) of each region and the latitudinal boundaries between them are shown.

**Figure 4 | Variability of the $C_{ANT}$ budget in the subpolar box during high NAO (1997) and low NAO (2002-2006).** Arrow and number formats are the same as in Figure 3, except for the numbers in green font that are the natural air-sea $CO_2$ fluxes in $PgC \cdot y^{-1}$, and in maroon font that are the air-sea heat flux in PW. Areal $C_{ANT}$ storage rates ($mol\text{-}C \cdot m^{-2} \cdot y^{-1}$) are also given. For 1997, the heat budget includes a heat accumulation rate of 0.10±0.05 PW.

**Supplementary Information**

**Atlantic Ocean $CO_2$ uptake reduced by weakening of the meridional overturning circulation**

Fiz F. Pérez[1], Herlé Mercier[2], Marcos Vázquez-Rodríguez[1], Pascale Lherminier[3], Anton Velo[1], Paula C. Pardo[1], Gabriel Rosón[4] and Aida F. Ríos[1]

[1] *Instituto de Investigaciones Marinas, IIM-CSIC, Vigo, Spain.* [2] *CNRS, Laboratoire de Physique des Océans, UMR6523, CNRS, Ifremer, IRD, UBO, Plouzané, France.* [3] *Ifremer, Laboratoire de Physique des Océans, UMR6523, CNRS, Ifremer, IRD, UBO, Plouzané, France.* [4] *Faculty of Marine Sciences, University of Vigo, Campus Lagoas-Marcosende, 36200 Vigo, Spain.*

## 1. Anthropogenic $CO_2$ computation and inventory estimate

We used three methods for computing anthropogenic $CO_2$ ($C_{ANT}$) from in situ measurements: the TTD (Transit Time Distribution[1]), TrOCA[2] and $\varphi C_T^o$ (refs 3,4) methods. On the basis of the variables needed to compute $C_{ANT}$, these methods can be classified into two groups: The carbon-based methods (TrOCA and $\varphi C_T^o$), which typically require measurements of $C_T$, $A_T$, oxygen, temperature, salinity and eventually nutrients, and the TTD method that uses CFC-11 or CFC-12 measurements as proxies of the anthropogenic $CO_2$ signal. A summary presentation of those methods of $C_{ANT}$ computation has been given in ref. 3. We applied the TrOCA and $\varphi C_T^o$ methods to the GLODAP and CARINA databases. The $C_{ANT}$ estimates obtained by applying the TTD method to the GLODAP dataset[1] were downloaded from the following website: https://jshare.johnshopkins.edu/dwaugh1/public_html/Cant/. The uncertainties in $C_{ANT}$ are ±6.2, ±5.2, and ±5.0 μmol kg$^{-1}$ for the TrOCA, $\varphi C_T^o$ and TTD methods, respectively[3]. They depend on the specific assumptions of each methodology and on the corresponding analytical errors of the variables involved.

To compute the $C_{ANT}$ inventories in the subtropical box, we first adapted the fields of [$C_{ANT}$] obtained from the CARINA/ GLODAP database to the WOA09 grid using a multi-parametric interpolation algorithm[5]. Second, we computed the specific (per unit area) inventories (Fig 1a) by vertically integrating the [$C_{ANT}$] on the WOA09 grid and, finally, we did a spatial (surface) integration to determine the inventories. The uncertainties in these inventories were calculated by randomly propagating over depth[3] a 5 μmol $kg^{-1}$ standard error of the $C_{ANT}$ estimate. The inventory uncertainties were equal to ±1 mol-C $m^{-2}$ and ±2 mol-C $m^{-2}$ when the vertical integration went down to 3000 m and 6000 m depths, respectively. For the subtropical box (surface area = $16.6 \cdot 10^{12}$ $m^2$), the estimated inventories are 17.3±0.3, 18.7±0.3 and 16.8±0.4 PgC for the TrOCA, $\varphi C_T^o$ and TTD methods respectively, that yield an average value of 17.6±0.6 PgC. In the subpolar box we relied on the $C_{ANT}$ inventories computed in Perez et al. (2010; ref. 6).

## 2. $C_{ANT}$ storage rate in the subtropical box

Based on previous works[7–9] we considered a transient steady state of the $C_{ANT}$ distribution in the subtropical NA. Accordingly, the storage rate of $C_{ANT}$ was computed from the inventory multiplied by the annual rate of increase $k_t$ ($C_{ANT}$ storage rate = $k_t$ * $C_{ANT}$ inventory). The value of $k_t$ (0.016±0.001 $y^{-1}$) was calculated as the rate of increase of [$C_{ANT}$] in the mixed layer divided by [$C_{ANT}$] in the mixed layer considering that the evolution of [$C_{ANT}$] in the winter mixed layer follows the exponential increase of atmospheric $CO_2$ (refs 8, 9). The storage rates in the subtropical box were estimated in 0.299±0.0045, 0.277±0.005 and 0.269±0.006 PgC·$y^{-1}$ by the TrOCA, $\varphi C_T^o$, and TTD methods, respectively. The value in the budget presented in Fig.3 was obtained as the mean value and standard error (0.280±0.011 PgC·$y^{-1}$) of the ensemble of storage rates from all three $C_{ANT}$ methods together. Also, $k_t$ was used as a rescaling factor of $C_{ANT}$ storage rates and $C_{ANT}$ transports to years 2004 and 1997, whenever these were reported for other years.

## 3. $C_{ANT}$ Storage rate in the subpolar box

Because the subpolar box includes areas of water mass formation[10,11], the assumption of a steady transient tracer distribution is not valid[9,12] there. This is mostly due to the fact that the thickness of the main water mass (LSW) in this region has a strong variability associated with the

NAO[10,11]. This variability drives strong changes in the $C_{ANT}$ storage rates[6,8,12] due to the formation of LSW during the period of low NAO compared to the exceptional convection activity during the period of high NAO[8]. For the budget presented in Fig. 4, we relied on ref. 6 who indicated a drop in the storage rate in the "OVIDE Box" from 0.054±0.006 $PgC \cdot y^{-1}$ during the high NAO period (1991-1997) to 0.026±0.004 $PgC \cdot y^{-1}$ during the low NAO period (1998-2006). These results are in agreement with those inferred from CFC data[8]. On average, the $C_{ANT}$ storage rate for the subpolar box referred to 2004 is 0.045±0.004 $PgC \cdot y^{-1}$ (Fig 3). The budget for the high NAO period in Fig. 4a was calculated by re-computing the storage rate in ref. 6 using the area of a subpolar box south-bounded by the FOUREX track. The storage rate was estimated at 0.083±0.008 $PgC \cdot y^{-1}$.

### 4. $C_{ANT}$ transports through the sills

The isopycnal $\sigma_0 = 27.80$ separates the northward flowing NA water masses entering the Nordic Seas [Eastern North Atlantic Central Water (ENACW), Modified North Atlantic Central Water (MNACW), Greenland-Iceland Inflow Water (GIIW)] in the upper layers from the southward flowing water masses [Denmark Strait Overflow Water (DSOW), Iceland Scotland Overflow Water (ISOW) and East Greenland Current (EGC)] in the lower layer (Supplementary Table 1). The volume transports and associated errors were taken from the literature[15].

### 5. $C_{ANT}$ storage in the Nordic Seas

Given the average $C_{ANT}$ inventory of 1.2 PgC estimated from chlorofluorocarbon data[13], a storage rate of $C_{ANT}$ of 0.018±0.004 $PgC \cdot y^{-1}$ was obtained using a $k_t$ of 0.016±0.001 $y^{-1}$ (refs 8, 9). This storage rate value is in agreement with a recent estimation[14].

**Supplementary Table 1 -** $C_{ANT}$ transports through the sills.

| **Water Mass** | **Volume Transport (Sv)** | **[$C_{ANT}$] (µmol kg$^{-1}$)** | **$C_{ANT}$ Transport referred to 2004 (kmol s$^{-1}$)** |
|---|---|---|---|
| DSOW | -3±1 | 30±3 | -89 |
| ISOW | -3±1 | 28±3 | -84 |
| EGC | -1.8±0.2 | 37±3 | -66 |
| ENACW | 3.85±1 | 49±4 | 189 |
| MNACW | 3.85±1 | 51±4 | 196 |
| GIIW | 0.8±0.2 | 40±3 | 32 |
| **Total** | 0.7±2.0 | | 166±51 kmol s$^{-1}$<br>0.063±0.019 PgC·y$^{-1}$ |

*EGC (East Greeland Current), ENACW (Eastern North Atlantic Central Water) MNACW (Modified North Atlantic Central Water) and GIIW (Greenland-Iceland Intermediate Water)*

The [$C_{ANT}$] in the upper layer were estimated assuming that surface waters are saturated with $CO_2$ (ref. 16). The [$C_{ANT}$] for the DSOW was taken from the literature[13] and [$C_{ANT}$] for the ISOW was estimated from water mass decomposition (Supplementary Table 2; refs 17, 18). The [$C_{ANT}$] data for the rest of the water masses flowing over the sills were taken from previous studies[13]. Additionally, since our study is referenced to years 1997 (high NAO) or 2004 (low NAO), $C_{ANT}$ transports over the sills were rescaled by applying the previously derived $k_t$ factor of 0.016 ±0.001 y$^{-1}$, and we obtained transports of 0.057±0.018 PgC·y$^{-1}$ and 0.063±0.019 PgC·y$^{-1}$ for 1997 and 2004, respectively. These results fully corroborate recent transport estimates (0.062±0.014 PgC·y$^{-1}$ for 2002; ref. 14).

**Supplementary Table 2.-** Water masses properties and [$C_{ANT}$] over the Nordic sills**.**

| **Water Mass** | **Mixing %** | **θ range (ºC)** | **θ avg. (ºC)** | **Salinity** | **[$C_{ANT}$] referred to 2004 (µmol kg$^{-1}$)** |
|---|---|---|---|---|---|
| NSAIW+NSDW | 50 | <0.4 | 0 | 34.885 | 10.9 |
| MEIW | 25 | <3 | 2 | 34.80 | 40.4 |
| MNAW | 25 | 8 | 7.75 | 35.15 | 49.2 |
| ISOW | 100 | | 2.44 | 34.93 | 28.0 |

*NSAIW (Norwegian Sea Arctic Intermediate Water), NSDW (Norwegian Sea Deep Water), MEIW (Modified East IcelandicWater) MNAW (Modified North Atlantic Water)*

## 6. Arctic Seas $C_{ANT}$ storage and transports

Based on earlier estimates[19], we considered an average value of 2.9±0.4 PgC for the $C_{ANT}$ inventory in the Arctic Seas referred to 2005. By applying the same $k_t$ factor of 0.016±0.001 $y^{-1}$, we estimated a $C_{ANT}$ storage rate of 0.043 $PgC\cdot y^{-1}$ referenced to 2004. The $C_{ANT}$ transport between the Arctic and Nordic Seas in 1991 was estimated to be 0.031±0.004 $PgC\cdot y^{-1}$ northward[20]. Rescaling this value to 2004, a $C_{ANT}$ transport of 0.039±0.008 $PgC\cdot y^{-1}$ was obtained. This result agrees with recent transport estimates of 0.040±0.019 $PgC\cdot y^{-1}$ referenced to 2002 (ref. 14). The $C_{ANT}$ transport through Davis Strait was neglected. The net $C_{ANT}$ transport from the Pacific to the Atlantic Ocean through the Bering Strait was obtained from previous works[21,22].

## 7. Transports and uncertainties at 25ºN

The seasonal variability of the MOC at 25°N has been recently evaluated[23] on the basis of the RAPID measurements. It has shown that the seasonal variability of the MOC is forced by the wind stress curl variability at the eastern boundary and affects the upper mid-ocean transport ($T_{UMO}$) in a narrow band close to the eastern boundary. The $[C_{ANT}]$ in this region ($[C_{ANT}]_{TUMO}$, Supplementary Table 3) was obtained from previous works[24,25] and the seasonal correction of $T_{CANT}$ was modeled as $\Delta T_{UMO}*[C_{ANT}]_{TUMO}$, where $\Delta T_{UMO}$ is seasonal transport anomaly. $\Delta T_{UMO}$ was estimated[23] at 0.9±0.9 and -2±0.9 Sv for the 1992 and 1998 cruises, respectively. The rescaled $C_{ANT}$ transports were hence computed applying the following equation:

$$T_{CANT}(2004) = (T_{CANT}(1992/1998) - \Delta T_{UMO}\,.[C_{ANT}]_{TUMO})\cdot (1+k_t)^{\Delta y}\cdot MOC_{RAPID}/MOC_{corr}$$

where $MOC_{corr}$ and $MOC_{RAPID}$ are the de-seasonalized and long-term averaged MOC (18.7±2.1 Sv) as given by ref. 23. Δy is the time lapse (in years) between 2004 and 1992 or 1998. The final uncertainties were computed as the standard deviation of an ensemble generated by random perturbations of the 1992/1998 $C_{ANT}$ transports, $\Delta T_{UMO}$, $[C_{ANT}]_{\Delta TUMO}$ and $k_t$. The value of 0.25±0.05 $PgC \cdot y^{-1}$ for $C_{ANT}$ transport at 25ºN is obtained as the mean between the 1992 and 1998 estimates, rescaled to 2004 and de-aliased from the seasonal variability. The most important contributions to the uncertainties are the initial uncertainties[24,25], while the rescaling of the MOC is practically negligible.

**Supplementary Table 3.-** Deseasonalized $C_{ANT}$ transport**.** **(**1 $PgC \cdot yr^{-1}$ = 2642 kmol/s)

| **Year** | **$C_{ANT}$ transport (kmol/s)** | **2004 $C_{ANT}$ transport (kmol/s)** | **$\Delta T_{UMO}$ (Sv)** | **$C_{ANT}$ $T_{UMO}$ ($\mu mol \cdot kg^{-1}$)** | **$MOC_{cor}$ (Sv)** | **$(1+ k_t)^{\Delta y}$** | **Long term 2004 $C_{ANT}$ transport ($PgC \cdot y^{-1}$)** |
|---|---|---|---|---|---|---|---|
| 1992 | 630±200 | 725±200 | 0.9±0.9 | 45±3 | 18.5 | 1.213±0.015 | 0.28±0.08 |
| 1998 | 449±159 | 610±160 | -2±0.9 | 51±3 | 18.1 | 1.066±0.005 | 0.23±0.06 |

8**. Transports and uncertainties at A25**

The MOC, heat, $C_{ANT}$ and natural $C_T$ transports across the A25 section are given in Supplementary Table 4. The natural $C_T$ was computed as the difference between measured (total) $C_T$ and $C_{ANT}$. The natural $C_T$ transports were used to establish a relationship between air sea fluxes of heat and natural $CO_2$ for the subpolar box (see Methods). The associated uncertainties in Supplementary Table 4 are the standard deviations of an ensemble of 100 tracer transport estimates obtained by random perturbations of the volume transports and tracer fields scaled using the error covariance matrix of the velocity field given by the inverse model[15] and the uncertainties in natural $C_T$ and $C_{ANT}$ concentrations (6 $\mu mol \cdot kg^{-1}$ each). The natural $C_T$ and $C_{ANT}$ transport uncertainties were equal to 0.026 and 0.014 $PgC \cdot yr^{-1}$, respectively. These uncertainties are very similar to those that would be obtained using the approximate method proposed by ref. 26.

The seasonal variability of the MOC along A25 was evaluated using the high-resolution DRAKKAR ocean general circulation model[27]. During the OVIDE cruises the seasonal anomaly was not significant (0.0±0.5) because these cruises were conducted in June, when the seasonal anomaly is at its minimum. On the contrary, the FOUREX occupation in September 1997 did need a seasonal correction of +2.0±0.5 Sv. The vertical gradient of the transport of [$C_{ANT}$] is not affected by the seasonal cycle[28] and we assumed that the seasonal variability of the vertical gradient of the transport of heat and natural $C_T$ is also negligible. So, we corrected for the seasonal variability of MOC transports from refs 29 and 30 by linearly rescaling the transports by the ratio <MOC>/MOC obtained in the model, where <MOC> is the annual value and MOC the monthly value (Supplementary Table 4).

**Supplementary Table 4.-** $C_{ANT}$ and natural $C_T$ transports through A25 section

| Cruise | MOC (Sv) | Heat (PW) | $C_{ANT}$ ($PgC\cdot yr^{-1}$) | Natural $C_T$ ($PgC\cdot yr^{-1}$) |
|---|---|---|---|---|
| **4X 1997** | 20.5 | 0.76±0.09 | 0.110±0.014 | -0.352±0.026 |
| **Ov 2002** | 16.2 | 0.44±0.05 | 0.077±0.014 | -0.207±0.026 |
| **Ov 2004** | 16.4 | 0.50±0.05 | 0.087±0.014 | -0.265±0.026 |
| **Ov 2006** | 11.2 | 0.29±0.05 | 0.058±0.014 | -0.079±0.026 |

## 9. Supplementary references


1. Waugh, D. W., Hall, T. M., McNeil, B. I., Key, R. & Matear, R. J. Anthropogenic $CO_2$ in the oceans estimated using transit time distributions. *Tellus B* **58**, 376–389 (2006).
2. Touratier, F., Azouzi, L. & Goyet, C. CFC-11, $\Delta^{14}C$ and $^{3}H$ tracers as a means to assess anthropogenic $CO_2$ concentrations in the ocean. *Tellus B* **59**, 318–325 (2007).
3. Vázquez-Rodríguez, M. *et al.* Anthropogenic carbon distributions in the Atlantic Ocean: data-based estimates from the Arctic to the Antarctic. *Biogeosciences* doi:10.5194/bg-6-439-2009 (2009).
4. Vázquez-Rodríguez, M., Padin, X. A., Ríos, A. F., Bellerby, R. G. J. & Pérez, F. F. An upgraded carbon-based method to estimate the anthropogenic fraction of dissolved $CO_2$ in the Atlantic Ocean. *Biogeosciences Discussions* doi:10.5194/bgd-6-4527-2009 (2009).
5. Velo, A. *et al.* A multiparametric method of interpolation using WOA05 applied to anthropogenic $CO_2$ in the Atlantic. *Sci. Mar.* **74**, 21–32 (2010).
6. Pérez, F. F. *et al.* Trends of anthropogenic $CO_2$ storage in North Atlantic water masses. *Biogeosciences* doi:10.5194/bg-7-1789-2010 (2010).
7. Keeling, C. D. & Bolin, B. The simultaneous use of chemical tracers in oceanic studies I. General theory of reservoir models. *Tellus* **19**, 566–581 (2010).
8. Steinfeldt, R., Rhein, M., Bullister, J. L. & Tanhua, T. Inventory changes in anthropogenic carbon from 1997–2003 in the Atlantic Ocean between 20°S and 65°N. *Glob. Biogeochem. Cycles* **23**, GB3010 (2009).
9. Tanhua, T. *et al.* Changes of anthropogenic $CO_2$ and CFCs in the North Atlantic between 1981 and 2004. *Glob. Biogeochem. Cycles* **20**, GB4017, 13 PP. (2006).
10. Yashayaev, I. & Dickson, B. Transformation and Fate of Overflows in the Northern North Atlantic. *Arctic–Subarctic Ocean Fluxes* 505–526 (2008).
11. Kieke, D. *et al.* Changes in the pool of Labrador Sea Water in the subpolar North Atlantic. *Geophys. Res. Lett.* **34**, L06605 (2007).
12. Pérez, F. F. *et al.* Temporal variability of the anthropogenic $CO_2$ storage in the Irminger Sea. *Biogeosciences* doi:10.5194/bg-5-1669-2008 (2008).
13. Jutterström, S. *et al.* Evaluation of anthropogenic carbon in the Nordic Seas using observed relationships of N, P and C versus CFCs. *Progress In Oceanography* **78**, 78–84 (2008).
14. Jeansson, E. *et al.* The Nordic Seas carbon budget: Sources, sinks, and uncertainties. *Glob. Biogeochem. Cycles* **25**, GB4010,16 PP. (2011).
15. Lherminier, P. *et al.* The Atlantic Meridional Overturning Circulation and the subpolar gyre observed at the A25-OVIDE section in June 2002 and 2004. *Deep-Sea Res. I* **57**, 1374–1391 (2010).
16. Tanhua, T., Olsson, K. A. & Jeansson, E. Tracer Evidence of the Origin and Variability of Denmark Strait Overflow Water. *Arctic–Subarctic Ocean Fluxes* 475–503 (2008).
17. Fogelqvist, E. *et al.* Greenland–Scotland overflow studied by hydro-chemical multivariate analysis. *Deep-Sea Res. I* **50**, 73–102 (2003).

18. Hansen, B. *et al.* The Inflow of Atlantic Water, Heat, and Salt to the Nordic Seas Across the Greenland–Scotland Ridge. *Arctic–Subarctic Ocean Fluxes* 15–43 (2008).
19. Tanhua, T. *et al.* Ventilation of the Arctic Ocean: Mean ages and inventories of anthropogenic $CO_2$ and CFC-11. *J. Geophys. Res.* **114**, C01002 (2009).
20. Anderson, L. G., Olsson, K. & Chierici, M. A carbon budget for the Arctic Ocean. *Glob. Biogeochemical Cycles* **12**, 455–465 (1998).
21. Macdonald, A. M., Baringer, M. O., Wanninkhof, R., Lee, K. & Wallace, D. W. R. A 1998–1992 comparison of inorganic carbon and its transport across 24.5°N in the Atlantic. *Deep-Sea Res. II* **50**, 3041–3064 (2003).
22. Mikaloff Fletcher, S. E. *et al.* Inverse estimates of anthropogenic $CO_2$ uptake, transport, and storage by the ocean. *Glob. Biogeochem. Cycles* **20**, GB2002 (2006).
23. Kanzow, T. *et al.* Seasonal Variability of the Atlantic Meridional Overturning Circulation at 26.5°N. *J. Clim.***23**, 5678–5698 (2010).
24. Rosón, G., Rios, A. F., Pérez, F. F., Lavin, A. & Bryden, H. L. Carbon distribution, fluxes, and budgets in the subtropical North Atlantic Ocean (24.5ºN). *J. Geophys. Res.* **108**, 3144 (2003).
25. Macdonald, A. M., Baringer, M. O., Wanninkhof, R., Lee, K. & Wallace, D. W. R. A 1998–1992 comparison of inorganic carbon and its transport across 24.5°N in the Atlantic. *Deep-Sea Res. II* **50**, 3041–3064 (2003).
26. Ganachaud, A., Wunsch, C., Marotzke, J. & Toole, J. Meridional overturning and large-scale circulation of the Indian Ocean. *J. Geophys. Res.* **105**, 26117–26,134 (2000).
27. Barnier, B. *et al.* Impact of partial steps and momentum advection schemes in a global ocean circulation model at eddy-permitting resolution. *Ocean Dyn.* **56**, 543–567 (2006).
28. Biastoch, A., Völker, C. & Böning, C. W. Uptake and spreading of anthropogenic trace gases in an eddy-permitting model of the Atlantic Ocean. *J. Geophys. Res.* **112**, C09017 (2007).
29. Lherminier, P. *et al.* Transports across the 2002 Greenland-Portugal Ovide section and comparison with 1997. *J. Geophys. Res.* **112**, C07003 (2007).
30. Gourcuff, C., Lherminier, P., Mercier, H. & Le Traon, P. Y. Altimetry combined with hydrography for ocean transport estimation. *J. Atmos. Oceanic. Technol.* **29** 1324-1336 (2011).

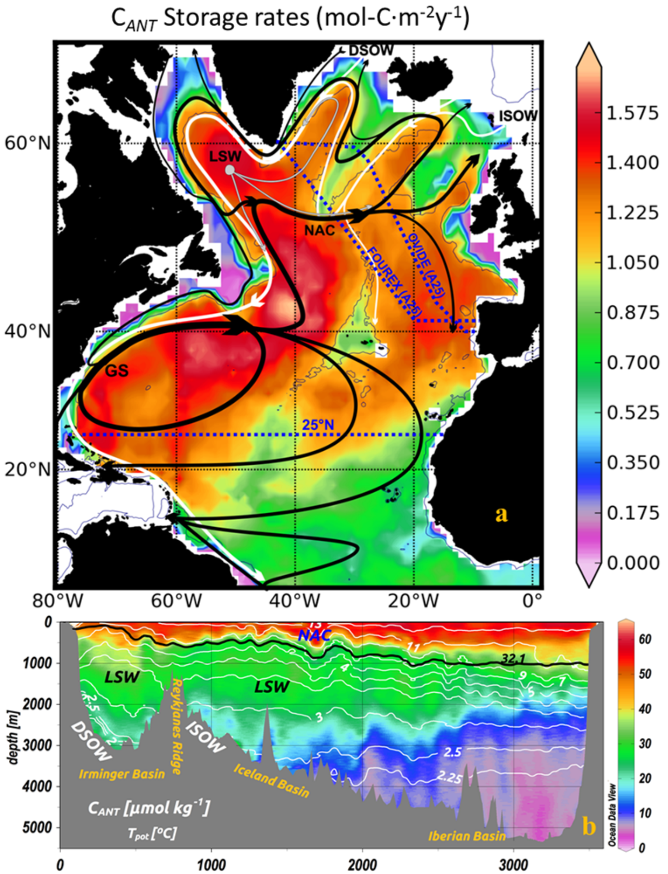

$C_{ANT}$ Storage rates (mol-C·m$^{-2}$y$^{-1}$)
DSOW
ISOW
LSW
NAC
GS
25°N
FOUREX (A25)
OVIDE (A25)
60°N
40°N
20°N
80°W
60°W
40°W
20°W
0°
1.575
1.400
1.225
1.050
0.875
0.700
0.525
0.350
0.175
0.000
a
NAC
LSW
LSW
32.1
DSOW
ISOW
Reykjanes Ridge
Irminger Basin
Iceland Basin
Iberian Basin
$C_{ANT}$ [µmol kg$^{-1}$]
$T_{pot}$ [°C]
depth [m]
Ocean Data View
b

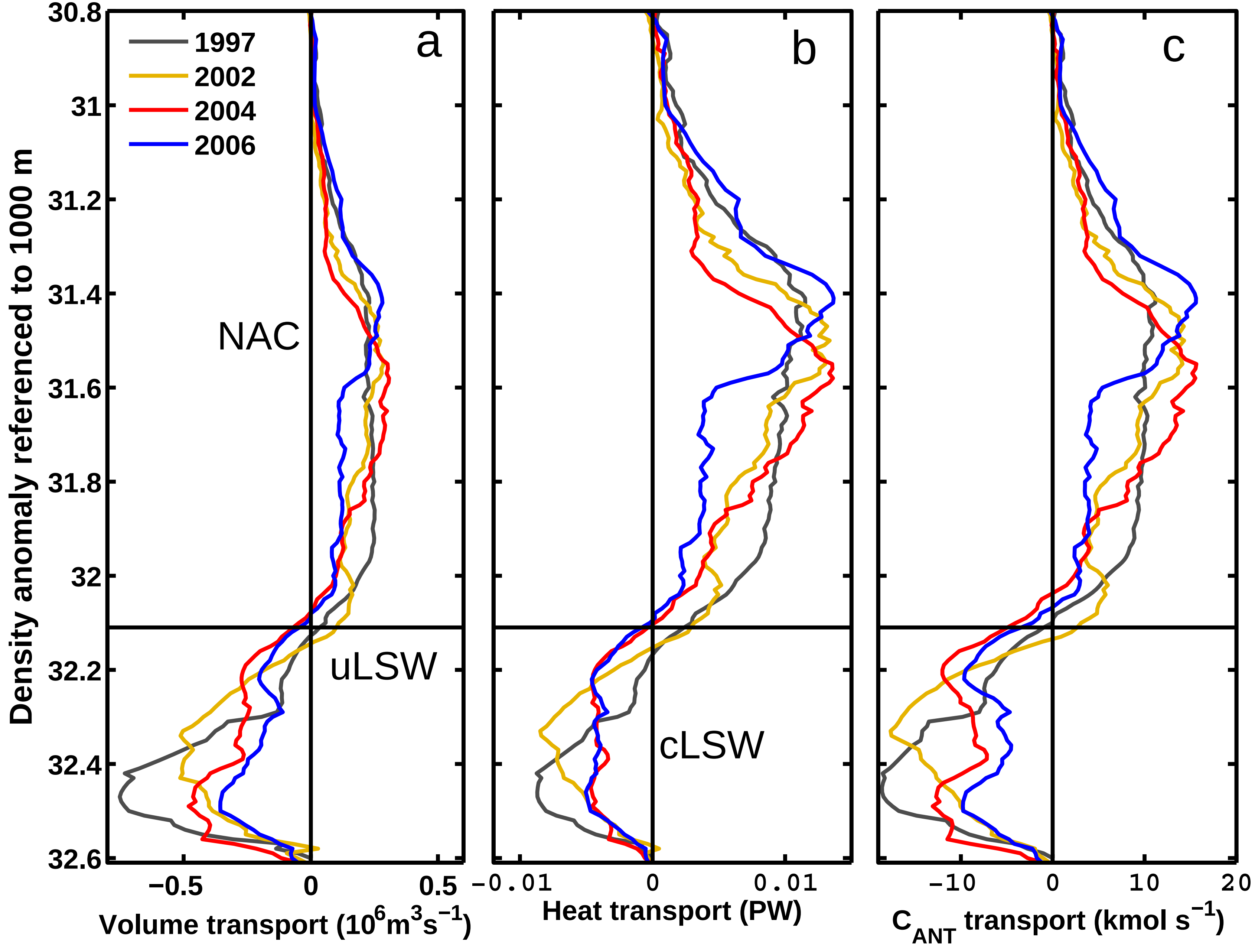

1997
2002
2004
2006
a
b
c
NAC
uLSW
cLSW
Density anomaly referenced to 1000 m
30.8
31
31.2
31.4
31.6
31.8
32
32.2
32.4
32.6
−0.5
0
0.5
Volume transport ($10^6 m^3 s^{-1}$)
−0.01
0
0.01
Heat transport (PW)
−10
0
10
20
$C_{ANT}$ transport (kmol $s^{-1}$)

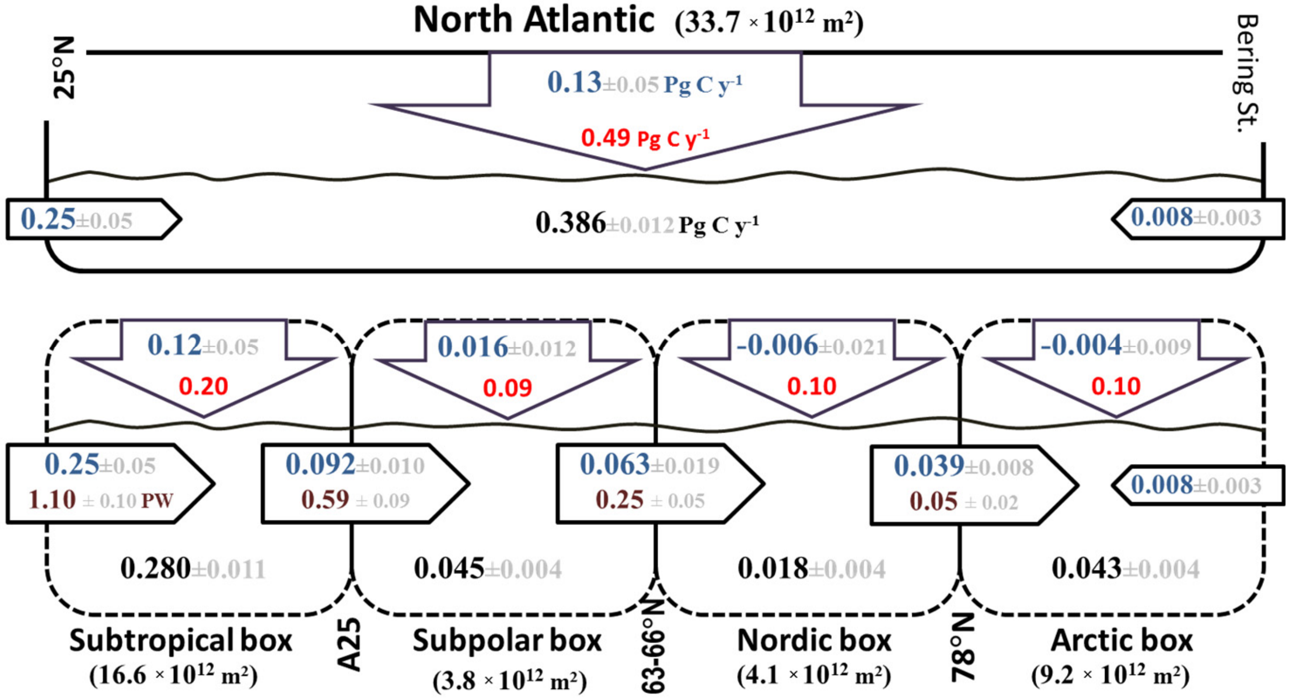
North Atlantic (33.7 × 10^12 m²)
25°N
Bering St.
0.13±0.05 Pg C y-1
0.49 Pg C y-1
0.25±0.05
0.386±0.012 Pg C y-1
0.008±0.003
0.12±0.05
0.20
0.016±0.012
0.09
-0.006±0.021
0.10
-0.004±0.009
0.10
0.25±0.05
1.10 ± 0.10 PW
0.092±0.010
0.59 ± 0.09
0.063±0.019
0.25 ± 0.05
0.039±0.008
0.05 ± 0.02
0.008±0.003
0.280±0.011
0.045±0.004
0.018±0.004
0.043±0.004
Subtropical box
(16.6 × 10^12 m²)
A25
Subpolar box
(3.8 × 10^12 m²)
63-66°N
Nordic box
(4.1 × 10^12 m²)
78°N
Arctic box
(9.2 × 10^12 m²)

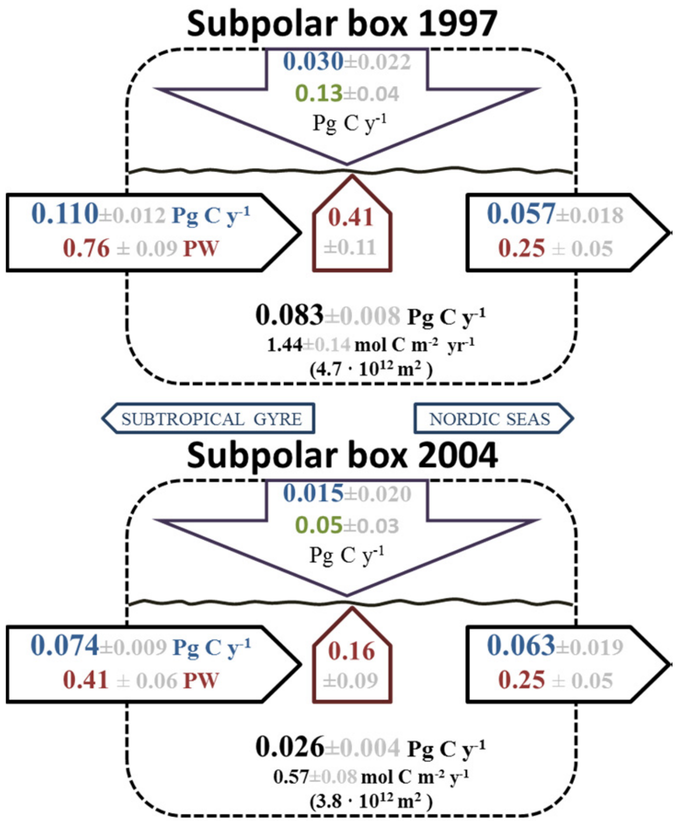
Subpolar box 1997
0.030±0.022
0.13±0.04
Pg C y-1
0.110±0.012 Pg C y-1
0.76 ± 0.09 PW
0.41
±0.11
0.057±0.018
0.25 ± 0.05
0.083±0.008 Pg C y-1
1.44±0.14 mol C m-2 yr-1
(4.7 · 10^12 m^2)
SUBTROPICAL GYRE
NORDIC SEAS
Subpolar box 2004
0.015±0.020
0.05±0.03
Pg C y-1
0.074±0.009 Pg C y-1
0.41 ± 0.06 PW
0.16
±0.09
0.063±0.019
0.25 ± 0.05
0.026±0.004 Pg C y-1
0.57±0.08 mol C m-2 y-1
(3.8 · 10^12 m^2)